Origin of the Optical Emission within the Cavity Mode of Coupled Quantum Dot-Cavity Systems

J. Suffczyński, A. Dousse, K. Gauthron, A. Lemaître, I. Sagnes, L. Lanco, J. Bloch, P. Voisin, and P. Senellart

Laboratoire de Photonique et Nanostructures, LPN/CNRS, Route de Nozay, 91460 Marcoussis, France
(Received 13 March 2009; published 6 July 2009)

The origin of the emission within the optical mode of a coupled quantum dot-micropillar system is investigated. Time-resolved photoluminescence is performed on a large number of deterministically coupled devices in a wide range of temperature and detuning. The emission within the cavity mode is found to exhibit the same dynamics as the spectrally closest quantum dot state. Our observations indicate that fast dephasing of the quantum dot state is responsible for the emission within the cavity mode. An explanation for recent photon correlation measurements reported on similar systems is proposed.

An individual semiconductor quantum dot (QD) coupled to an optical cavity mode is a promising system in view of practical implementation of efficient single photon sources [1], nanolasers [2], as well as remote quantum bit entanglement [3]. Early experiments of solid state cavity quantum electrodynamics (CQED) relied on the random possibility of finding a QD spectrally and spatially resonant with a single cavity mode [4–6]. In these first demonstrations, the yield of the fabrication process was very small and hindered the possibility of performing systematic investigations. Recently, many technological advances like deterministic QD-cavity coupling [7,8], tuning techniques , and electrical pumping of the devices [11] have enabled a better control of the system. As a result, the number of optical studies of solid state CQED has increased [12–14] and it now appears that the system cannot simply be described in the framework of the Jaynes-Cumming model as for CQED with atoms [15]. Indeed, when studying the emission of coupled QD-cavity devices, unexpected questions arise, whether the system is in the weak coupling regime (Purcell effect) [12] or strong coupling regime [13,14]. Why, in the situation where the spectral detuning between the quantum dot and the optical mode is much larger than the mode linewidth, emission is still mostly observed at the mode energy? Why, even though the emission within the cavity mode presents a quasi-Poissionian statistics, is it strongly anticorrelated with the QD emission [12–14]? To what extent do dephasing processes influence the emission properties in solid state CQED?

In the present work, we study the emission dynamics of coupled QD-pillar cavities in the weak coupling regime. Each pillar embeds a single QD deterministically coupled to its fundamental optical mode. Time-resolved photoluminescence measurements are carried out in a quantum dot-mode detunings range extending up to three mode linewidths. The emission within the cavity mode is found to present the same dynamics as the spectrally closest QD state, in a wide temperature range and independently of the detuning sign. This is observed whether the decay of the QD state emission is given by its radiative lifetime or is driven by scattering processes. When two states of the

same QD are equally detuned from the cavity mode, the emission within the mode presents the same decay as the spectrally wider QD state. These observations indicate that the emission within the cavity mode is driven by fast dephasing processes [16,17], in accordance with recent theoretical proposals [18–21]. Our results also provide an overall explanation for recent photon correlation measurements reported on similar systems [12,13].

Pillar microcavities were fabricated using a planar microcavity constituted by 20 (24) pairs of $Al_{0.1}Ga_{0.9}As/Al_{0.95}Ga_{0.05}As$ Bragg mirrors. The cavity exhibits a quality factor of 4500 and embeds a layer of self-organized InAs/GaAs QDs. Rapid thermal annealing of the sample (30 s at 850 °C) allows reducing the spatial density of QDs emitting at the planar cavity mode energy to less than 1 μm^{-2} by blueshifting the overall quantum dot distribution [22]. Micropillars containing an individual QD spectrally and spatially matched to the microcavity fundamental mode are fabricated with the single-step *in situ* lithography technique detailed in Ref. [8]. The deterministic coupling between a single low energy QD and the pillar fundamental mode allows neglecting the influence of other QDs in a wide range of detunings. Pillar diameters range from 1.5 μm to 2.3 μm. The sample is placed in a cold finger cryostat. The photoluminescence (PL) is excited nonresonantly at 1.59 eV with a pulsed Ti:sapphire laser. The same microscope objective is used to focus the laser beam on the pillars and to collect the emission which is sent to a spectrometer. The emission is then detected by a CCD camera with a 150 μeV spectral resolution or by a streak camera for time-resolved analysis with a resolution of 20 ps.

Time-resolved PL is measured on seven pillars. The detuning Δ between the cavity mode and the QD state is tuned over a wide range by varying the temperature. Change of the temperature modifies not only the magnitude of the Purcell effect on the QD state, but also carrier scattering toward the QD higher energy states. As a result, various and complex dependences can be observed when studying the emission dynamics of the QD emission line as a function of temperature. We investigate the emission dynamics within the cavity mode for these various situ-

ations and start with illustrating of our findings by present-
ing the measurements on two pillars A and B.

Pillar A presents a 1.7 μm diameter and a quality factor
$Q = 1300$. It embeds a QD in its center experiencing a
Purcell factor of $F_P = 7$. Figure 1(a) shows the time
integrated PL spectra from pillar A taken in the 10 to
50 K temperature range. The emission lines are identified
through power and temperature dependent measurements
as coming from recombination of neutral exciton (X),
biexciton (XX) and charged exciton (CX) confined in the
same QD, as well as emission within the cavity mode (M).
At 10 K, the fundamental mode M is resonant to XX. The
streak camera image recorded at $T = 10$ K is shown in
Fig. 1(b). The radiative cascade between the XX and X
state is seen as a delay of the X signal rise with respect to
XX signal. The XX decay time is $\tau_{XX} = 135 \pm 30$ ps,
much shorter than the typical 1 ns decay time in these
QDs, showing the strong Purcell effect experienced by the
XX. When increasing temperature, the XX-M detuning as
well as the XX decay time increase. Measurements per-
formed on QD transitions well detuned from the cavity
mode show no change of the decay times between 10 and
45 K. As a result, the increase of the XX decay time for
pillar A can fully be attributed to the gradual quenching of
the Purcell effect below 45 K.

When the XX-M detuning is large enough, the decay
time of the emission within the cavity mode is extracted
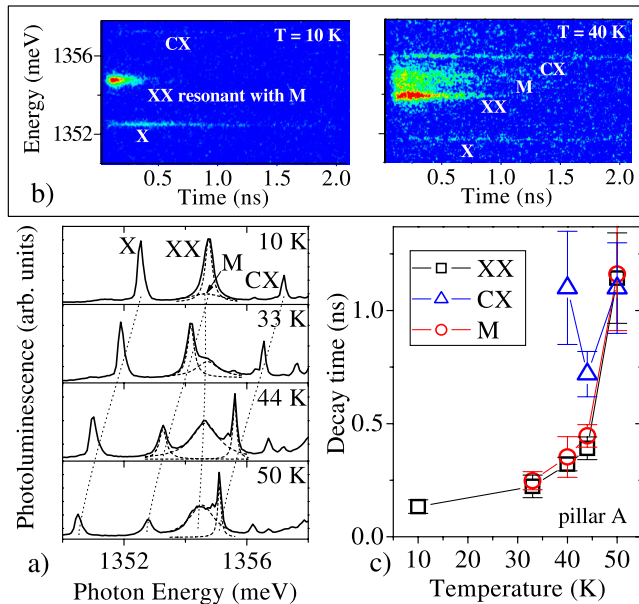from the streak camera images. The decay times of the M

and XX lines are plotted as a function of temperature in
Fig. 1(c). Remarkably, in the whole 10–45 K temperature
range, both the XX and M lines present the same decay
time. The same behavior is observed on each pillar for
which the emission dynamics of the QD state is determined
by its radiative decay. We now show that the same behavior
is also observed when the QD state dynamics is no longer
governed by its radiative decay.

Indeed, around 50 K, scattering of carriers out off the
QD fundamental state leads to an increase of the decay
time of the QD states [23]: nonresonantly created carriers
are still rapidly captured into the QD, but confined carriers
are scattered to the s-p nonradiative states and the decay
time of the QD line is no longer determined by its radiative
lifetime. Influence of these scattering processes is seen on
the CX line which decay shortens due to the Purcell effect
between 40 and 44 K, but increases at 50 K even though
CX is closer to resonance with the cavity mode [Fig. 1(c)].

To illustrate the properties of the mode emission at
elevated temperature, we present the measurements per-
formed on pillar B (diameter 2.3 μm, $\gamma_M = 0.45$ meV,
$Q = 3000$, $F_P = 8$) for which the X-M resonance occurs
around 57 K. Figure 2(b) shows the X decay time as a
function of temperature and X-M detuning. Although the
signal from X state is greatly enhanced due to Purcell effect
[see Fig. 4(a)] when X is tuned to resonance with M, no

FIG. 1 (color online).   (a) Time integrated emission spectra of
pillar A taken at temperatures T between 10 and 50 K. Excitation
power 0.25 μW. Dotted curves help following the spectral
position of the X, CX, XX, and M lines with temperature.
(b) Streak camera images (emission intensity as a function of
energy and time) measured on pillar A at $T = 10$ K and $T =$
40 K. (c) Emission decay time for XX, CX, and M lines as a
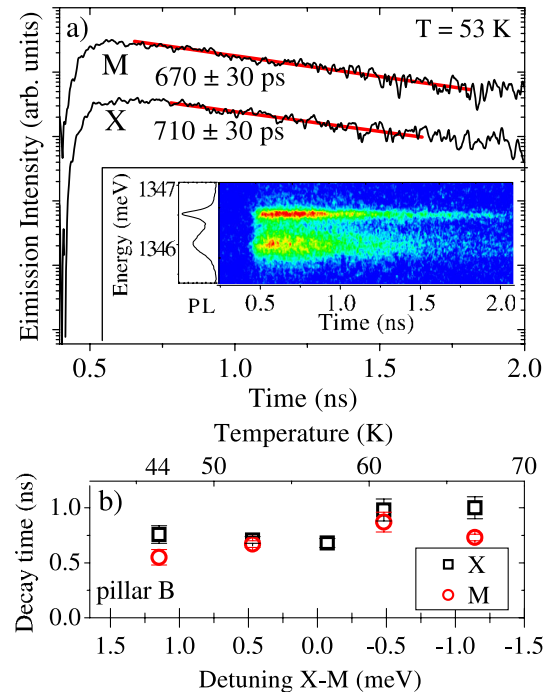function of T between 10 and 50 K.

FIG. 2 (color online).   (a) Emission intensity as a function of
time at X and M wavelengths measured on pillar B at $T = 53$ K.
The curves have been vertically shifted for clarity. Decay times
obtained from a monoexponential fit are indicated. Inset: corre-
sponding streak camera image and PL spectrum. (b) Emission
decay time for X and M lines plotted versus X-M detuning
(bottom axis) and temperature (top axis).

shortening of the X emission decay is observed. This is because the observed X emission decay time is governed by the lifetime of the carriers in higher energy states above 50 K. However, as for pillar A, in the whole temperature range, the decay time of the emission within the cavity mode is very close to the decay time of the excitonic line.

The strong correlation between the decay time within the cavity mode and the QD emission line observed on both, A and B, pillars is further investigated on five other pillars, presenting Purcell factor between 7 and 14, in a range of detunings up to 3 mode linewidths and for temperatures between 10 and 70 K. Figure 3 shows the decay time of the emission within the cavity mode versus the decay time of the QD state closest in energy, collecting the results on all seven pillars. The experimental points are remarkably located on the diagonal for QD decay times ranging from 250 ps to 2 ns. This observation demonstrates that the emission within the cavity mode arises from the spectrally closest QD state. In Ref. [13], observation of antibunching between the QD emission and the emission within the cavity mode suggested that a single quantum emitter was responsible for the emission at both QD and mode energies. Our measurements further show that there is no delay between the rise of emission at QD energy and M energy [Figs. 1(b) and 2(a)], evidencing that the mechanism responsible for the strong QD emission at the mode
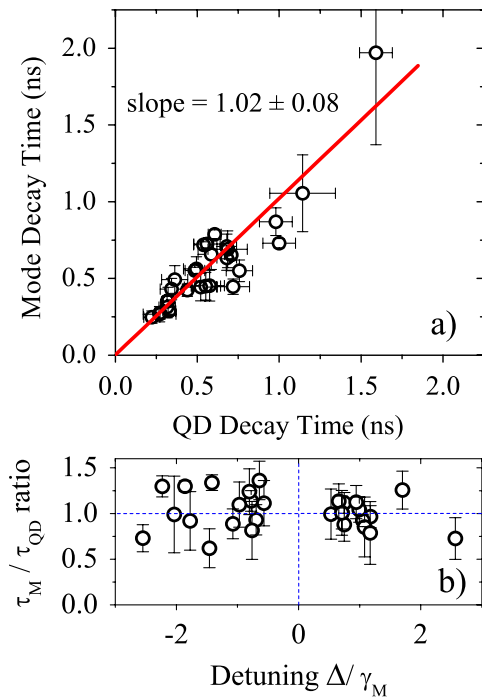
energy takes place on a time scale much shorter than the QD radiative lifetime. Figure 3(b) shows the ratio τ_M/τ_{QD} plotted versus the QD-M detuning normalized by the mode linewidth γ_M for each micropillar. Experimental points are scattered around unity with no dependence on the detuning Δ value or sign.

In the framework of the Jaynes-Cumming Hamiltonian, when the emitter is monochromatic as compared to the mode line, the emission is mainly peaked at the QD energy whatever the QD-M detuning is. Emission at the energy of the cavity mode is essentially negligible outside the QD-M crossing region. However, in solid state systems, it is well known that coupling with acoustic phonons [16] as well as surrounding carriers [17] can lead to fast dephasing of the QD emission line. In a recent theoretical work, Naesby and co-workers [18] have investigated the issue of unexpectedly strong emission within the cavity mode in the case the strong coupling regime. They show that when pure dephasing broadens the QD line, the emission at the energy of the cavity mode is greatly enhanced. In this framework, the emission dynamics is expected to be the same both at QD and M energies, as observed here. For a strong dephasing of the QD state, the emission is expected to mainly take place at the mode energy, independently of the detuning Δ in the large detuning range. The fraction of emission within M is calculated to decrease close to QD-M resonance.

Figure 4(a) plots the emission intensity within the mode as a function of detuning with the X line, evidencing a strong decrease close to resonance. This behavior is observed for each resonance X, XX or CX with the cavity mode, further confirming the major role played by fast dephasing. The ratio of the emission intensity within the M to overall (X and M) emission intensity is plotted in Fig. 4(b) showing that 80% of emission takes place within the mode for large detunings. Close to resonance, this ratio
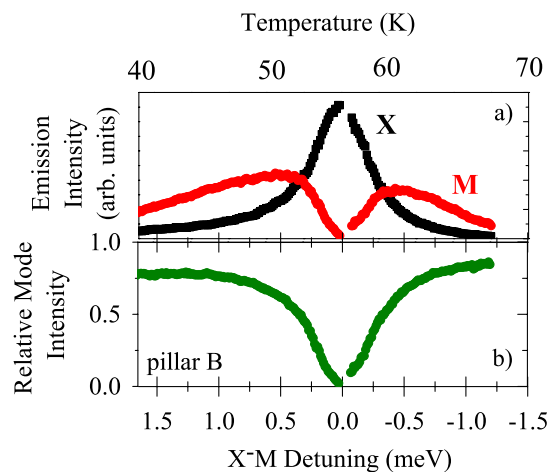

FIG. 3 (color online). (a) Decay time of the emission within cavity mode τ_M as a function of the emission decay time for the spectrally closest QD state τ_{QD} measured on seven different devices for more than 30 temperatures. Free parameter linear fit yielding the 1.02 ± 0.08 slope is shown. (b) The ratio τ_M/τ_{QD} as a function of QD-M detuning Δ normalized by mode linewidth γ_M of each pillar.

FIG. 4 (color online). (a) Intensity of X (black) and M (red) emission lines measured on pillar B. (b) Ratio of emission intensity within the mode to the overall (X plus M) emission intensity. The plots are versus X-M detuning (bottom axis) and temperature T (top axis).

decreases down to 0.01. This decrease is much stronger in our experiment than calculated in Ref. [18]. However, Naesby *et al.* treat the case of strong coupling regime when the QD broadening due to pure dephasing exceeds the mode linewidth. In this case, the emission intensity within each line is equal at resonance, so that the ratio goes to 0.5. Further theoretical investigations are needed to quantitatively describe the influence of fast dephasing in the weak coupling regime, when the QD linewidth remains smaller than the mode linewidth.

As one would expect, the observation of similar decay times for the emission from a QD state and the emission within the cavity mode falls when the detuning is very large. As seen in Fig. 1(b) at 40 K, the cavity mode presents the same decay as the XX line, closest in energy, while the decay at the strongly detuned exciton energy is longer. In the framework of QD emission within the mode mediated by dephasing processes, we note that when the cavity mode lies between two transitions of the coupled QD, the emission within the cavity mode is fed by a combination of the two states. This effect is clearly seen on pillar A at 44 K. The CX is slightly spectrally closer to the mode than the XX state at this temperature, yet the decay of the emission within the mode is mostly driven by the XX decay. Indeed, as can be seen on the spectra in Fig. 1(a), the XX presents a much larger linewidth (290 μeV) than the CX (<150 μeV): this difference in dephasing results in a stronger contribution of XX to the emission within the mode. In Fig. 3(a), the decay time at M energy is plotted as a function of the spectrally closest QD state decay time with no consideration of the other QD states and their emission linewidths: most of the off diagonal experimental points reflect measurements where the mode lies between two QD lines presenting different dephasing. Finally, when the cavity mode is strongly detuned from any quantum dot state, we accordingly observe that the emission at the mode energy presents a decay time different from any particular QD line as reported in Ref. [13].

The above considerations allow us to propose an explanation for the photon correlation experiments reported in [13], where some apparent contradiction was seen. While a strong anticorrelation between the X emission and the emission within the cavity mode was observed suggesting that both emissions arose from the same quantum emitter, autocorrelation measurements performed on the emission within the cavity mode revealed almost no antibunching [13]. Under nonresonant excitation and in the large detuning range where these experiments have been performed, the emission within the cavity mode results from the sum of various contributions corresponding to fast dephasing of several states of the same QD. In this framework, cross correlation between M and X is a sum of correlations between X, CX, XX emissions and X emission, weighted by respective value of detuning, dephasing, and intensity of each line of the QD. In continuous wave excitation, all the correlation functions contributing to this sum (autocorrelation X-X and cross correlations CX-X and XX-X) reveal

an anticorrelation at zero delay time [24] and for negative delays, so that their sum also exhibits $g^{(2)}(\tau = 0) \sim 0$ and anticorrelation for negative delay. On the contrary, for positive delay, X-X autocorrelation exhibits antibunching and CX-X and XX-X cross correlations bunching, which explains the strong asymmetry in the X-M correlation histogram reported in Ref. [13]. The observation of almost no antibunching in M-M autocorrelation under pulsed excitation is explained in a similar way. M-M autocorrelation is the sum of all possible autocorrelations and cross correlations between all the states of the same QD. In pulsed excitation measurements, each cross correlation within the radiative cascade contributes to the zero delay peak of the histogram and decreases the level of antibunching.

In conclusion, emission dynamics of deterministically coupled quantum dot-pillar microcavity systems bring strong evidence that the emission within the cavity mode results from fast dephasing of the QD state, in agreement with recent theoretical works [18,19]. Specifically, emission within the cavity mode is driven by the closest state of the QD. When two states are similarly detuned from the cavity mode, the emission at the mode energy is driven by the spectrally widest quantum state. We note that thanks to deterministic coupling, the influence of other QDs embedded in the pillar is negligible. Therefore, the devices enable unambiguous investigations without the need for a selective QD excitation.

[1] Ch. Santori *et al.*, Nature (London) **419**, 594 (2002).
[2] S. Strauf *et al.*, Phys. Rev. Lett. **96**, 127404 (2006).
[3] C. Y. Hu *et al.*, Phys. Rev. B **78**, 085307 (2008).
[4] T. Yoshie *et al.*, Nature (London) **432**, 200 (2004).
[5] J. P. Reithmaier *et al.*, Nature (London) **432**, 197 (2004).
[6] E. Peter *et al.*, Phys. Rev. Lett. **95**, 067401 (2005).
[7] A. Badolato *et al.*, Science **308**, 1158 (2005).
[8] A. Dousse *et al.*, Phys. Rev. Lett. **101**, 267404 (2008).
[9] S. Strauf *et al.*, Appl. Phys. Lett. **88**, 043116 (2006).
[10] A. Laucht *et al.*, arXiv:0810.3010v2.
[11] C. Böckler *et al.*, Appl. Phys. Lett. **92**, 091107 (2008).
[12] M. Kaniber *et al.*, Phys. Rev. B **77**, 161303(R) (2008).
[13] K. Hennessy *et al.*, Nature (London) **445**, 896 (2007).
[14] D. Press *et al.*, Phys. Rev. Lett. **98**, 117402 (2007).
[15] A. Auffèves *et al.*, Phys. Rev. A **77**, 063833 (2008).
[16] E. Peter *et al.*, Phys. Rev. B **69**, 041307(R) (2004).
[17] A. Berthelot *et al.*, Nature Phys. **2**, 759 (2006).
[18] A. Naesby *et al.*, Phys. Rev. A **78**, 045802 (2008).
[19] A. Auffèves *et al.*, Phys. Rev. A **79**, 053838 (2009).
[20] S. Hughes and P. Yao, Opt. Express **17**, 3322 (2009).
[21] M. Yamaguchi *et al.*, Opt. Express **16**, 18 067 (2008).
[22] W. Langbein *et al.*, Phys. Rev. B **70**, 033301 (2004).
[23] H. Yu *et al.*, Appl. Phys. Lett. **69**, 4087 (1996).
[24] E. Moreau *et al.*, Phys. Rev. Lett. **87**, 183601 (2001).